Layout optimization for multi-bi-modulus materials system under multiple load cases

Jiao Shi [1], Jing Cao [1], Kun Cai [1, 2], Zhenzhong Wang [1a], Qing-Hua Qin [2a]

[1.] *College of Water Resources and Architectural Engineering, Northwest A&F University, Yangling 712100, China*

[2.] *Research School of Engineering, the Australian National University, Acton, ACT 2601, Australia*

[a)] Authors to whom correspondence should be addressed. Email address: wangzz0910@163.com; Qinghua.qin@anu.edu.au

Abstract: An optimization model is presented for obtaining optimal layout of multiple bi-modulus materials systems under multiple load cases (MLC). In the optimization model, the objective function is the linearly weighted structural compliance under MLC. The bi-modulus materials in a finite element are replaced by isotropic materials according to the stress state of that element. The equivalent mechanical properties of an element are expressed as the power-law function of the volume fractions (design variables) and moduli of the solid phases. Numerical experiments are presented to verify the validity and efficiency of the present algorithm. The effects of factors including the bi-modulus behavior of materials, the load directions and the weighting schemes of MLC are also investigated numerically.

Keywords: Topology optimization; Bi-modulus materials; Multi-material structures; Multiple load cases; SIMP

1. Introduction

During recent decades, topological optimization has gained considerable attention in both theoretical research and practical applications [1-3]. Due to their complexity, topology optimization problems with large numbers of design variables are still the most challenge task in the structural optimization field. Several optimization schemes have been reported, including the homogenization-based method [4], the SIMP method (solid isotropic material with penalization) [5-7], the ESO (evolutionary structural optimization) method [8,9], and the level set method [10,11]. Topology optimization has been used widely in the design of engineering structures such as MEMS [12], acoustics [13],

crashworthiness [14], fluidics [15], bone structures [16], and heat conduction [17].

In practical engineering, a structure is often under multiple loads (MLs). To apply topology optimization on such structures, Díaz and Bendsøe [18] developed an optimization model with a single objective function using a linear weighting scheme for MLs. Similarly, Bendsøe et al. [19] addressed the design of material properties and material distribution in structures under MLC. Luo et al. [20] presented a hybrid fuzzy-goal multi-objective programming scheme for topology optimization that considered both static and dynamic loadings. Sui at al. [21] suggested an independent continuous mapping method for solving the topology optimization problems of a continuum under MLs. Balamurugan et al. [22] used a genetic algorithm for the topology design of structures under MLs.

Most of the work above focused on a continuum with single material only. Topological design with multi-phase materials is more complex than traditional 0-1 design of structures with only one solid phase. For solving topology optimization problems with multi-phase materials, the level set method was developed [23-25]. Other methods including the ESO method [26], phase-field method [27], and pseudo-sensitivities scheme [28] have also been proposed.

Few of the works mentioned above have considered optimization of the layout of bi-modulus materials. Nevertheless, bi-modulus materials that have different tensile and compressive moduli along the same direction are very common in engineering. For example, materials such as rubber, concrete, cast iron, graphite, foam materials, masonry, bone, alloys, and ropes/membranes exhibit bi-modulus behavior. Due to the stress-dependency of bi-modulus materials, deformation analysis of bi-modulus structures is more complex than that of structures with isotropic materials [29]. Achtziger [30] considered the bi-modulus effect on the final topology of a truss and found that the final structure under tension was obviously different from that under compression. Chang et al. [31] approximated the original piecewise linear stress–strain curve of a bi-modulus material with a derivable nonlinear curve for the topological design of a tension-only or compression-only material. Cai [32] solved the tension-only or compression-only design using a modified SIMP method, in which the tension-only or compression-only material is

replaced with an isotropic material. Querin et al. [33] used orthotropic materials to replace the original bi-modulus material according to the local stress state in topology optimization of truss-like structures. Cai et al. [34] suggested a sampler scheme for finding the optimal topology of a continuum structure with one bi-modulus material.

In the present work, topology optimization of multi-phase bi-modulus materials under MLs is studied. Numerical examples are presented showing the applicability and efficiency of the proposed algorithm.

2. Methodology

2.1. Statement of linear elasticity problem

For a linear elastic structure, the basic equations read

$$\begin{aligned} &-\nabla\cdot\boldsymbol{\sigma}(\boldsymbol{u})=\boldsymbol{f} \quad in\Omega\ , \\ &\boldsymbol{\varepsilon}(\boldsymbol{u})=\frac{1}{2}\left[\nabla\boldsymbol{u}+(\nabla\boldsymbol{u})^{T}\right], \\ &\boldsymbol{\sigma}(\boldsymbol{u})=\boldsymbol{D}:\boldsymbol{\varepsilon}(\boldsymbol{u}), \end{aligned} \tag{1}$$

and the corresponding boundary conditions are:

$$\begin{aligned} &\boldsymbol{u}=\boldsymbol{u}_0 \qquad on\Gamma_1, \\ &\boldsymbol{\sigma}(\boldsymbol{u})\boldsymbol{n}=\boldsymbol{T} \qquad on\Gamma_2. \end{aligned} \tag{2}$$

where Γ_1 and Γ_2 are Dirichlet condition and Neumann condition respectively and $\Gamma_1\cup\Gamma_2=\partial\Omega$. $\Omega\subset R^2$ or R^3 is the design domain. $\boldsymbol{\varepsilon}$ and $\boldsymbol{\sigma}$ are the strain and stress tensors respectively. $\boldsymbol{f}$ is the body force vector, $\boldsymbol{u}$ is the displacement field, $\boldsymbol{u}_0$ is the prescribed displacement on Γ_1, and $\boldsymbol{T}$ is boundary force on Γ_2. $\boldsymbol{D}$ is the elasticity tensor.

2.2. SIMP approach for optimization of layout of multiple materials

Topology optimization based on the density-like method of the SIMP approach [6] is adopted. In the density-like method, the equivalent modulus of a composite material is calculated using the material interpolation scheme of the moduli and volume fractions of the components in the composite. For manufacturing, the final design should have only one component material in one element, and interfaces between component materials

should be on common boundaries between elements.

For a [0, 1] design of only one component material using the SIMP method, the interpolation for material modulus in an element is defined as

$$E^{(1)}\left(\rho_{1,j}\right)=\rho_{1,j}^{p}\cdot E_1+\left(1-\rho_{1,j}^{p}\right)\cdot E_{\text{void}}=\rho_{1,j}^{p}\cdot E_1 \tag{3}$$

where $E^{(1)}$ means the equivalent modulus of a composite with one solid material and voids. $\rho_{1,j}\in[0,\ 1]$ are the volume fraction, a design variable of the *j*-th element, E_1 is the elastic modulus of the solid phase, and p is the penalization parameter, typically p=3.

When the composite has m types of solid with the moduli of $E_1, E_2, \ldots, E_m$, $(E_1 > E_2 >, \ldots, > E_m)$, $E^{(m)}$ can be given based on the interpolation scheme,

$$E^{(m)}\left(\rho_{1,j},\rho_{2,j},...,\rho_{m\text{-}1,j}\right)=\rho_{m-1,j}^{p}\cdot E^{(m-1)}+\left(1-\rho_{m-1,j}^{p}\right)\cdot E_m\,. \tag{4}$$

In this equation, $\rho_{i,j}$ is the summation of the volume fractions of the first *i* types of solid in the composite element, and $\rho_{m,j}$=1.0. This interpolation scheme is used in the present study.

2.3. Optimization model

For the stiffness design of a continuum with multiple bi-modulus materials under MLC, the optimization model reads

$$\begin{aligned}
&\textbf{Find} \quad \left\{\rho_{i,j}\middle| i\in\{1,2,\cdots,m\},\ j\in\{1,2,\cdots,n\}\right\}\\
&\textbf{min} \quad c=\sum_{l=1}^{N_{LC}} w_l\cdot\overline{c_l},\\
&\textbf{s.t.} \quad \sum_{j=1}^{n}\rho_{r,j}\cdot v_j=V_0\cdot\sum_{i=1}^{r} f_i,\\
&\qquad \sum_{l=1}^{N_{LC}} w_l=1.0,\\
&\qquad \overline{\boldsymbol{K}}_l\cdot\overline{\boldsymbol{U}}_l=\boldsymbol{F}_l,\quad (l=1,2,\cdots,N_{LC}),\\
&\qquad 0<\rho_{\min}\le\rho_{1,j}\le\rho_{2,j}\le\cdots\le\rho_{m,j}=1,\\
&\qquad 0<w_l,\ (l=1,2,\cdots,N_{LC}).
\end{aligned} \tag{5}$$

where the design variable $\rho_{i,j}$ is the volume fraction of the *i*-th component material in

the *j*-th element. The objective function, c, is the weighted mean compliance of structure under the multiple load cases ($\overline{c_l}$, $(l=1, 2, \cdots, N_{LC})$). N_{LC} is the number of loading cases. $\boldsymbol{F}_l$ and $\overline{\boldsymbol{U}}_l$ denote the global nodal force and displacement vector in the *l*-th load case respectively. $\overline{\boldsymbol{K}}_l$ is the final global stiffness matrix of a structure with many bi-modulus materials, and can be calculated using the well-established finite element formulation [35-38], "*n*" and "*m*" are respectively the total number of finite elements and the number of solid materials in the design domain. v_j is the *j*-th element volume, f_i is the *i*-th material volume fraction, V_0 denotes the volume of the design domain. $\rho_{\min}$ is the minimum value of relative densities. To avoid singularity of the stiffness matrix $\boldsymbol{K}_l$, here we set $\rho_{\min}=0.001$.

2.4. Material replacement scheme for bi-modulus material

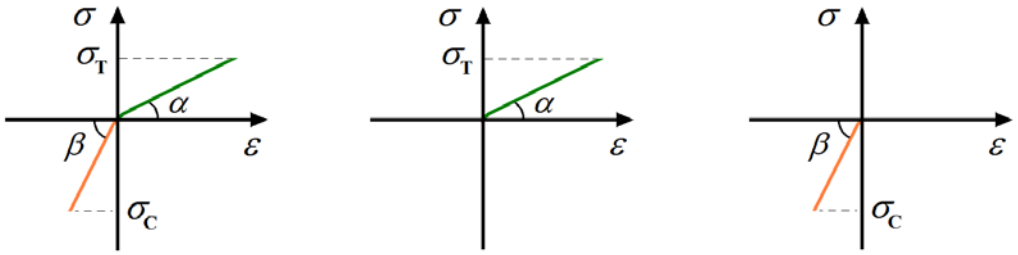

(a) Bi-modulus material (b) Tension-only material (c) Compression-only material

Fig. 1. Stress–strain curves for a common bi-modulus material and two special cases

Fig. 1a shows the stress–strain curve of a bi-modulus material with tensile modulus of $E^{\mathrm{T}}=\tan\alpha$ (green line) and compressive modulus of $E^{\mathrm{C}}=\tan\beta$ (orange line). The stress–strain curve is piecewise linear if $\alpha\neq\beta$. $\alpha=\beta$ means that the material is degenerated into an isotropic material. If $\beta=0$, the material is a tensile-only material (Fig. 1b). If $\alpha=0$, the material is a compressive-only material (Fig. 1c). σ_{T} and σ_{C} are the allowable stresses of the material under tension and compression, respectively. σ_{T}

and σ_{C} are usually different.

To represent the difference between tension and compression performance, the ratio between E^{T} and E^{C} is defined as

$$R_{\mathrm{TCE}} = \frac{E^{\mathrm{T}}}{E^{\mathrm{C}}}. \tag{6}$$

In the deformation analysis of a structure with bi-modulus materials, many structural reanalyses could be required due to the nonlinearity of materials. However, the nonlinearity here has some particular features. For example, the bi-modulus material appears isotropic when it is under pure compression or under pure tension. When the material is in a complex stress state, e.g., the first principal stress is positive but the third is negative, the eigen pairs of the elasticity tensor depend on the direction and value of the second principal stress. Hence, in a structure with an optimal load-transmission path (LTP), most of the structure is under a simple stress state. At the junction of adjacent parts, however, the material may be transverse isotropic because of its complex stress state. This condition implies that we can use an appropriate isotropic material to replace the bi-modulus material during structural deformation analysis. The difference in structural stiffness caused by such replacement can be modified step by step. The merit of material replacement is that the structural deformation analysis becomes a linear analysis after replacement. The modification of the local stiffness difference can be performed during the topology optimization process. Two aspects must therefore be given in detail for the material replacement scheme. The first is selection of the isotropic material that will replace the bi-modulus material in structural deformation analysis. The second is modification of the local stiffness due to material replacement.

2.4. 1 Selection of isotropic material for local replacement

For a given element in a design domain, σ_s and ε_s ($s = 1, 2, 3$) denote the principal stresses and principal strains.

(1) If $0 \geq \sigma_1 > \sigma_2 > \sigma_3$, the compressive modulus of the bi-modulus material should be the same as that of the isotropic material;

(2) If $\sigma_1 > \sigma_2 > \sigma_3 \geq 0$, the tensile modulus of the bi-modulus material should be the same as that of the isotropic material;

(3) If the element is under a complex stress state, i.e., $\sigma_1 \cdot \sigma_3 < 0$, the elastic modulus depends on the comparison between the values of the tension strain energy density (SED) and compression SED, which considers the influence of the second principal stress.

Mathematically, the modulus of the isotropic material to replace the *i*-th bi-modulus material can be obtained from the equation:

$$E_{i,j} = \begin{cases} E_{i,j}^{\mathrm{T}}, & \text{if } SED_{\mathrm{T}} > SED_{\mathrm{C}}, \\ E_{i,j}^{\mathrm{C}}, & \text{if } SED_{\mathrm{T}} < SED_{\mathrm{C}}, \\ \max\left(E_{i,j}^{\mathrm{T}}, E_{i,j}^{\mathrm{C}}\right), & \text{others.} \end{cases} \tag{7}$$

where the tension SED (SED_{T}) and compression SED (SED_{C}) are determined by the equations:

$$SED_{\mathrm{T}} = \sum_{l=1}^{N_{LC}} w_l \cdot \left(\sum_{G=1}^{N_G} \sum_{s=1}^{3} \left(\frac{1}{4N_G} \left(|\sigma_s| + \sigma_s \right) \cdot \varepsilon_s \right)_G \right), \tag{8}$$

$$SED_{\mathrm{C}} = \sum_{u=1}^{t} w_u \cdot \left(\sum_{G=1}^{N_G} \sum_{s=1}^{3} \left(\frac{-1}{4N_G} \left(|\sigma_s| - \sigma_s \right) \cdot \varepsilon_s \right)_G \right). \tag{9}$$

where N_G is the number of Gaussian integral points in the element.

2.4.2 Modification of local stiffness

Accurate deformation of a structure depends on an accurate global stiffness matrix, which is formed by using the local (element) stiffness matrix. When a difference appears after material replacement, the local stiffness matrix of the element with the isotropic material is different from that of the same element with the original bi-modulus material. To eliminate the difference, under the same stress state, the same element should have the same strain energy density before and after replacement. According to this principle, we can calculate the modification factor by comparing the SEDs before and after replacement.

Under a complex stress state at the *k*-th iteration, the SED of the element with the

new isotropic material is

$$SED_{j,k} = \sum_{l=1}^{N_{LC}} \left(w_l \cdot \sum_{G=1}^{N_G} \sum_{s=1}^{3} \left(\frac{1}{2N_G} \sigma_s \cdot \varepsilon_s \right)_G \right) \tag{10}$$

and the effective SED of the element with the original bi-modulus materials is

$$SED_{j,k}^{\text{effective}} = \sum_{i=1}^{m} \left\{ \gamma_i \cdot \sum_{l=1}^{N_{LC}} \left(w_l \cdot \sum_{G=1}^{N_G} \sum_{s=1}^{3} \left(\frac{1}{2N_G} \text{sign}_i(\sigma_s) \cdot \sigma_s \cdot \varepsilon_s \right)_G \right) \right\}_{j,k} . \tag{11}$$

where $\gamma_i = \rho_i - \rho_{i\text{-}1}$ is the volume fraction of the *i*-th material in the element.

The value of the $\text{sign}_i(\cdot)$ can be calculated using either Eq.(11) or Eq.(12) below.

(a) If the element has ***compressive moduli*** at the (*k*-1)-th iteration and ***tensile moduli*** should be used at the current (*k*-th) iteration, the value of the $\text{sign}_i(\cdot)$ is

$$\text{sign}_i(\sigma_s) = \begin{cases} 1 & \text{if } \sigma_s \geq 0, \\ R_{\text{TCE}}^{(i)} & \text{if } \sigma_s < 0. \end{cases} \tag{12}$$

where $R_{\text{TCE}}^{(i)}$ is the moduli ratio of the *i*-th bi-modulus material.

(b) If the element has ***tensile moduli*** at the (*k*-1)-th iteration and ***compressive moduli*** should be used at the current *k*-th iteration, the value of the $\text{sign}_i(\cdot)$ is

$$\text{sign}_i(\sigma_s) = \begin{cases} 1 & \text{if } \sigma_s \leq 0, \\ \left(R_{\text{TCE}}^{(i)} \right)^{-1} & \text{if } \sigma_s > 0. \end{cases} \tag{13}$$

By comparing Eqs.(10) and (11), we find that the two SEDs are identical when the element is under pure tension or pure compression. If the element is under a complex stress state, the two SEDs are usually different. The difference of the local effective stiffness of the *j*-th element at the *k*-th iteration is defined as

$$M_f = \max\left(10^{-6}, \frac{SED_{j,k}^{effective}}{\max\left(SED_{j,k}, 10^{-10} \right)} \right). \tag{14}$$

The stiffness matrix of the *j*-th element with the "new" isotropic materials can be given as [36,39,40]

$$\boldsymbol{k}_j = \int_{v_j} \boldsymbol{B}_j^T \cdot \boldsymbol{D}_j \cdot \boldsymbol{B}_j \text{d}v . \tag{15}$$

where $\boldsymbol{B}_j$ is the displacement–strain matrix, and $\boldsymbol{D}_j$ is the elasticity matrix of the *j*-th

element.

The modified stiffness matrix of the element is defined as

$$\bar{\boldsymbol{k}}_j = M_f \boldsymbol{k}_j = \int_{v_j} \boldsymbol{B}_j^T \left(M_f \cdot \boldsymbol{D}_j \right) \boldsymbol{B}_j \mathrm{d}v . \tag{16}$$

For the *l*-th loading case, the mean compliance of the structure with bi-modulus materials (in Eq.(5)) can be obtained, i.e.,

$$\overline{c_l} = \sum_{j=1}^{n} \boldsymbol{u}_j^T \left(M_f \boldsymbol{k}_j \right) \boldsymbol{u}_j = \sum_{j=1}^{n} M_f \cdot \boldsymbol{u}_j^T \cdot \boldsymbol{k}_j \cdot \boldsymbol{u}_j \tag{17}$$

2.5. Optimization procedure

In the present study, the Method of Moving Asymptotes (MMA) [41] is adopted to solve the optimization problem defined in Eq.(5). The partial differential equations for structural deformation expressed in Eq.(1) with boundaries in Eq.(2) are solved by the commercial software ANSYS 12.0. In the following numerical examples, the initial elastic moduli of the materials in the elements are the same as the tensile modulus of the first solid material (Material 1). All the initial design variables are considered to be equal. The MMA procedure contains the following steps:

Step 1) Build a finite element model of the structure, initiate parameters in optimization, and let $i = 1$;

Step 2) Find the deformation fields of the structure under MLC by finite element analysis;

Step 3) Calculate the SED, tension SED, compression SED and the local effective SED of each element in the design domain;

Step 4) Chose the moduli of the materials in each element by comparing tension SED and compression SED; calculate the value of M_f for each element under a complex stress state;

Step 5) Compute the values of the objective and constraint functions and their sensitivities;

Step 6) Update the design variables for each element by the MMA optimizer [41];

Step 7) Check the convergence: if the termination criterion is not satisfied, return to

Step 2, else go to Step 8;

Step 8) Judge, if $i < m-1$, then, $i = i+1$, return to Step 2, otherwise, go to Step 9;

Step 9) Save and stop.

The termination criterion is either that the iteration number is greater than 100 or that the change of compliance of the structure satisfies the condition:

$$\left| \frac{c_{k-t} - c_k}{c_k} \right| \le \eta, \quad \left(t \in \{1, 2, 3, 4, 5\} \right). \tag{18}$$

where η is the algorithm tolerance.

3. Examples and Discussion

In this section, numerical examples are considered and assessed by the present algorithm. The code is compiled by combining software MATLAB and ANSYS (V12.0) [42]. In all examples, four-node quadrilateral plane stress elements are employed in the finite element analysis. In optimization, the objective is to minimize the compliance of the structure. The Poisson's ratios of materials in all examples are set to be 0.2.

3.1. Example 1: Validity assessment

The structure shown in Fig. 2a is a cantilever beam with dimensions 0.7m × 0.4m × 0.02m, and is meshed with 120 × 60 elements. The left side of the structure is fixed. There are two solids and a void phase in the structure. The material tensile moduli of the two solids are 80GPa and 40GPa, respectively. $R_{\mathrm{TCE}}^{(1)} = 2 > 1$ and $R_{\mathrm{TCE}}^{(2)} = 0.5 < 1$. Volume fractions of the two solids and void phase are 0.12, 0.12, and 0.76, respectively.

The structure is under two loading cases, i.e., P_1=2000N in the first case, P_2=2000N in the second case. P_1 is applied on the center of the right side of the structure. P_2 is applied on the center of the design domain (Fig. 2a). The weighting scheme is $w_1 = 0.2$ and $w_2 = 0.8$.

From Fig. 2b, we find that Material 1 (red) is mainly under tension and Material 2 (green) is under compression. If we consider the components in the final structure as LTP,

Material 1 is mainly on tensile LTPs and Material 2 on compressive LTPs. From the R_{TCE} values of the two materials we know that the two materials have higher stiffness under the current loading states with $w_1 = 0.2$ and $w_2 = 0.8$. Briefly, the moduli of the two materials are the same, i.e., 80 GPa, in the final structural topology, a result that can also be obtained by using single phase topology optimization with an approach such as the SIMP method. With a different weighting scheme, we believe that the amount of material supporting the two forces would be different. But the optimal materials layout must have the property stated above, that the majority of the materials in the final structure should have higher moduli in order to decrease structural compliance. It is concluded that the correctness of the algorithm is verified.

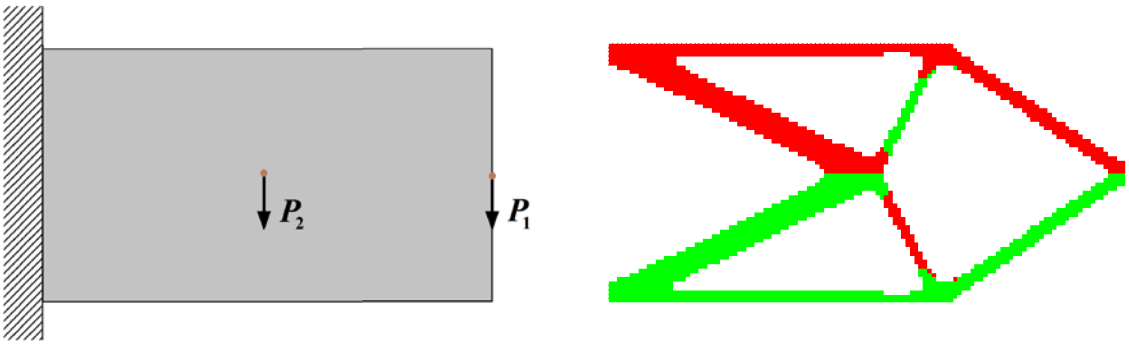

(a) Initial design (b) $w_1 = 0.2, w_2 = 0.8$

Fig. 2. Structural and optimal shape under different MLC (Material 1: red, Material 2: green, void: white)

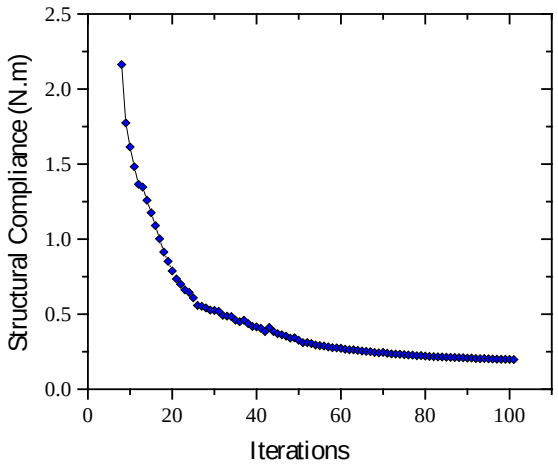

Fig. 3. Iteration histories of the mean compliance of structure under two loading cases with three

different weighting schemes (η=0.01)

Fig. 3 demonstrates that the structural compliance approaches 0.19782 N.m after 101 iterations for the structure under MLC with the weighting scheme of $w_1 = 0.2$ and $w_2 = 0.8$. Because no internal iteration occurs within each update of the design variables, only 101 structural deformation analyses are needed. Hence, the present algorithm has acceptable efficiency during optimization.

3.2. Example 2: Effect of R_{TCE} on final materials layouts

The design domain is shown in Fig. 4 with the dimensions 1.6m × 0.5m × 0.01m. The structure is modelled with 160 × 50 elements. Two loading cases are considered. In the first case, P_1=2000N is applied at the point "K_1". In the second case, two concentrated forces P_2=2000N are applied at two points "K_2". The design domain contains two solid materials and one void phase, with the volume fractions 0.16, 0.16, and 0.68, respectively. The tensile moduli of the two solids (Material 1 and Material 2) are 100GPa and 50GPa, respectively. If the two materials are bi-modulus materials, the values of R_{TCE} of the two solids are 2 and 0.5, respectively. For comparison, the optimal layouts of the two isotropic solids are also given.

Three weighting schemes are considered:

(1) $w_1 = 1, w_2 = 0,$ (only P_1 is active),

(2) $w_1 = 0, w_2 = 1,$ (only P_2 is active),

(3) $w_1 = 0.5, w_2 = 0.5.$

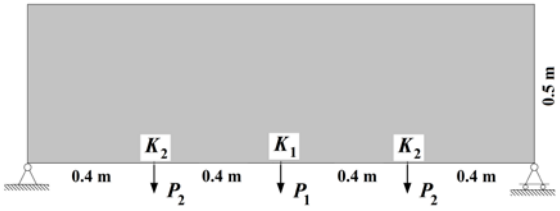

Fig. 4. Initial design domain

When the structure is only under the load P_1, the final layout of the two solid bi-modulus materials (Fig. 5a) is different from the traditional design, that is, the isotropic materials layout. In Fig. 5a, Material 1 is under pure tension because its tensile modulus is greater than the compressive modulus ($R_{\mathrm{TCE}}^{(1)} = 2 > 1$). Almost all of Material 2 is under compression due to its compressive modulus being greater than the tensile modulus ($R_{\mathrm{TCE}}^{(2)} = 0.5 < 1$). In Fig. 5b, the interfaces between the two isotropic solids are more complex than in Fig. 5a.

When the structure is subjected only to P_2, the bi-modulus materials layout is also different from that of isotropic materials. The interface of the two bi-modulus solids (Fig. 5c) is also simpler than that between two isotropic solids (Fig. 5d). Hence, when the moduli of the two solids are clearly different, the complex bi-modulus behavior of the materials does not imply that they have complex interface, which would be difficult for manufacturing.

Under the two loading cases, the final materials layouts (Fig. 5e, f) are different from those in the structure under a single load. Material 1 (bi-modulus) is still mainly under tension, and most of Material 2 is still under compression (Fig. 5e).

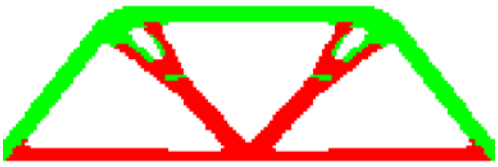

(a) $w_1 = 1, w_2 = 0$, bi-modulus materials

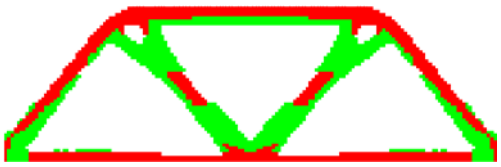

(b) $w_1 = 1, w_2 = 0$, isotropic materials

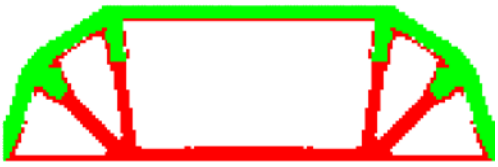

(c) $w_1 = 0, w_2 = 1$, bi-modulus materials

(d) $w_1 = 0, w_2 = 1$, isotropic materials

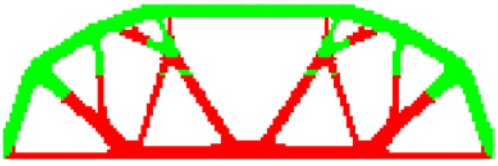

(e) $w_1 = 0.5, w_2 = 0.5$, bi-modulus materials

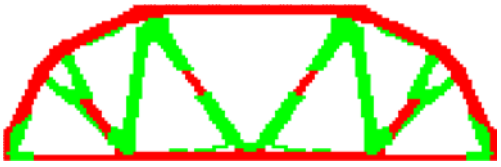

(f) $w_1 = 0.5, w_2 = 0.5$, isotropic materials

Fig. 5. Final materials distribution in the structure for different cases (Material 1: red, Material 2: green, void: white)

3.3. Example 3: Effect of load directions

The dimensions of the structure used in this example are 1.6m × 0.4m × 0.01m. The structure is simply supported and the finite element mesh is 160 × 40. There are two solids (Material 1 and Material 2) and one void phase in the structure. The two solids have the tensile moduli of 100GPa and 50GPa, respectively. They are bi-modulus materials, and the values of the R_{TCE} of the two solids are 2 and 0.5, respectively. The volume fractions of the three phases are 0.2, 0.2, and 0.6, respectively.

The structure is under two loading cases with two vertical concentrated forces, P_1 and P_2, applied separately on the centers of the upper and lower sides of structure. Both forces have a magnitude of 2000N. In different schemes, the directions of the two forces may be different. Three schemes are considered (see the uppermost layer of Fig. 6).

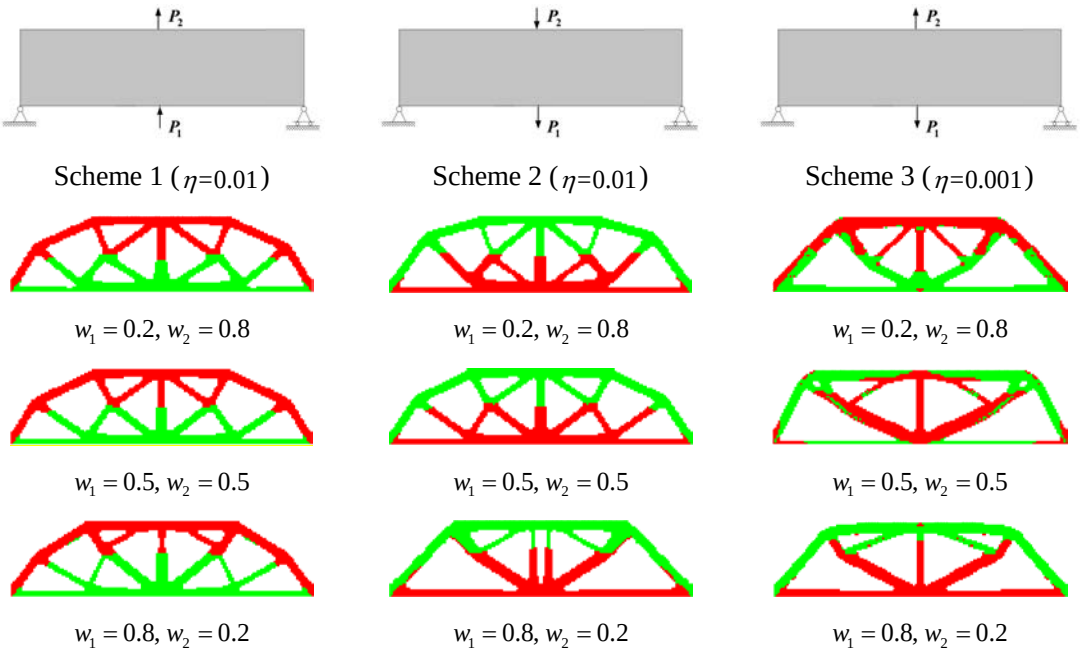

Fig. 6. The final materials layouts in the structure under different schemes (Material 1: red, Material 2: green, void: white)

The results for scheme 1 (the left column) demonstrate that Material 1 (red) is mainly under tension for two loading cases, and Material 2 is under compression when the directions of the two forces are vertical upward. The reason is that the tensile modulus of Material 1 is greater than the compressive modulus ($R_{\mathrm{TCE}}^{(1)} = 2 > 1$), whereas Material 2 has higher compressive stiffness ($R_{\mathrm{TCE}}^{(2)} = 0.5 < 1$).

This situation changes when the directions of the two forces are vertical downward (scheme 2). In the central column (scheme 2), Material 1 layouts are near the lower side of the beam rather than near the upper side as in scheme 1.

If the directions of the two forces are different, as in scheme 3, the layouts of the two bi-modulus materials are clearly different from those in schemes 1 and 2. Moreover, the locations of Material 1 in the final structure depend on the weighting coefficients of the two load cases. For example, Material 1 layouts are near the upper side when $w_1 = 0.2, w_2 = 0.8$ (P_2 has higher influence on structural compliance than P_1), in the central area of the structure when $w_1 = 0.5, w_2 = 0.5$, or near the bottom when $w_1 = 0.8, w_2 = 0.2$.

This phenomenon does not occur in either scheme 1 or scheme 2. The weighting coefficients of the two loading cases have only a slight influence on the positions of the material interfaces in scheme 1. Only when $w_1 = 0.8, w_2 = 0.2$ is the topology of the structure different from the other topologies in scheme 2.

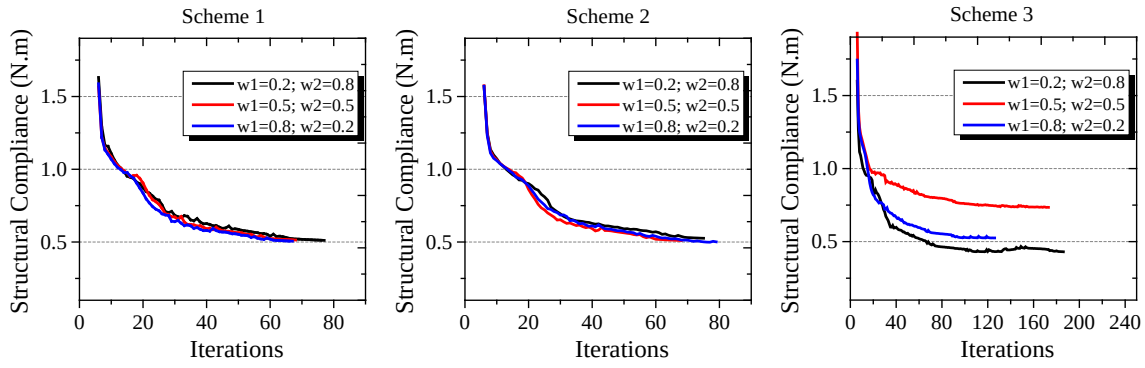

Fig. 7. Iteration histories of the mean compliance of the structure under MLC with different load directions/schemes.

Table 1. Final iterations and values of the objective function (Obj) (or mean compliance) of the structure with different load direction schemes.

	Scheme 1 (η=0.01)		Scheme 2 (η=0.01)		Scheme 3 (η=0.001)	
Weighting	Iterations	Obj (N.m)	Iterations	Obj (N.m)	Iterations	Obj (N.m)
$w_1 = 0.2, w_2 = 0.8$	77	0.51137	75	0.52606	186	0.43058
$w_1 = 0.5, w_2 = 0.5$	68	0.51368	68	0.51055	168	0.73453
$w_1 = 0.8, w_2 = 0.2$	67	0.50587	79	0.50121	121	0.52510

In Fig. 7 and Table 1, we find that the number of iterations does not exceed 200 in the 9 different cases. With the same weighting coefficients, namely $w_1 = 0.2, w_2 = 0.8$, the optimal value of structural compliance is different for different load directions. Simultaneously, the layout differences among the three schemes are attributable to the bi-modulus behavior of the two materials under loads with different directions [43].

4. Conclusions

Using the algorithm presented in this study to achieve optimal layout of multiple bi-modulus materials in a continuum under MLC, three numerical tests are considered. From the numerical results some remarkable conclusions are drawn.

(1) The computational cost of the present algorithm is very close to that of simple single material layout optimization by the SIMP method.

(2) In a stiffness design, materials with higher modulus should be laid out on the main LTPs. When the differences among the moduli of bi-modulus materials are not great, on the tensile LTPs, materials with R_{TCE}>1 are usually laid out. Materials with R_{TCE}<1 are usually laid out on the compressive LTPs.

(3) The final layouts of bi-modulus materials are sensitive to the values of R_{TCE} and the load conditions. Under the same loading conditions, the interfaces between bi-modulus materials may be clearer than those between isotropic materials.

(4) The optimal layout of bi-modulus materials depends on the force directions (forward and reverse).

Hence, the present algorithm is applicable and effective for analyzing the performance of structures with many bi-modulus materials and under MLC.

Acknowledgement

Financial support from the National Natural Science Foundation of China (Grant No. 51179164) and the Australian Research Council (Grant No. DP140103137) is acknowledged.

References

1. Bendsøe, M.P., Sigmund, O.: Topology optimization: theory, methods and applications. Springer, Berlin (2003)
2. Eschenauer, H.A., Olhoff, N.: Topology optimization of continuum structures: A review. Applied Mechanics Reviews **54**(4), 331-390 (2001)
3. Cai, K., Luo, Z.J., Qin, Q.H.: Topology optimization of bi-modulus structures using the concept of bone remodeling. Engineering Computations **31**(7), 1361-1378 (2014)
4. Bendsøe, M.P., Kikuchi, N.: Generating optimal topologies in structural design using a homogenization method. Computer Methods in Applied Mechanics and Engineering **71**(2), 197-224 (1988)
5. Rozvany, G., Zhou, M., Birker, T.: Generalized shape optimization without homogenization. Structural Optimization **4**(3-4), 250-252 (1992)
6. Zhou, M., Rozvany, G.I.N.: The COC algorithm, Part II: Topological, geometrical and generalized shape optimization. Computer Methods in Applied Mechanics and Engineering **89**(1-3), 309-336 (1991)
7. Qin, Q.H., He, X.: Variational principles, FE and MPT for analysis of non-linear impact-contact problems. Computer Methods in Applied Mechanics and Engineering **122**(3), 205-222 (1995)
8. Xie, Y.M., Steven, G.P.: A simple evolutionary procedure for structural optimization. Computers & Structures **49**(5), 885-896 (1993)
9. Huang, X., Xie, Y.-M.: A further review of ESO type methods for topology optimization. Structural and Multidisciplinary Optimization **41**(5), 671-683 (2010)
10. Wang, M.Y., Wang, X., Guo, D.: A level set method for structural topology optimization. Computer Methods in Applied Mechanics and Engineering **192**(1), 227-246 (2003)
11. Allaire, G., Jouve, F., Toader, A.-M.: Structural optimization using sensitivity analysis and a level-set method. Journal of Computational Physics **194**(1), 363-393 (2004)
12. Kota, S., Joo, J., Li, Z., Rodgers, S.M., Sniegowski, J.: Design of compliant mechanisms: applications to MEMS. Analog Integrated Circuits and Signal Processing **29**(1-2), 7-15 (2001)
13. Dühring, M.B., Jensen, J.S., Sigmund, O.: Acoustic design by topology optimization. Journal of Sound and Vibration **317**(3-5), 557-575 (2008)
14. Forsberg, J., Nilsson, L.: Topology optimization in crashworthiness design. Structural and Multidisciplinary Optimization **33**(1), 1-12 (2007)
15. Gersborg-Hansen, A., Sigmund, O., Haber, R.B.: Topology optimization of channel flow problems. Structural and Multidisciplinary Optimization **30**(3), 181-192 (2005)
16. Shi, J., Cai, K., Qin, Q.H.: Optimal Mass Distribution Prediction for Human Proximal Femur with Bi-modulus Property. MCB: Molecular & Cellular Biomechanics **11**(4), 235-248 (2014)
17. Gersborg-Hansen, A., Bendsøe, M.P., Sigmund, O.: Topology optimization of heat conduction problems using the finite volume method. Structural and Multidisciplinary Optimization **31**, 251-259 (2006)

18. Diaz, A., Bendsøe, M.: Shape optimization of structures for multiple loading conditions using a homogenization method. Structural Optimization **4**(1), 17-22 (1992)
19. Bendsøe, M.P., Díaz, A.R., Lipton, R., Taylor, J.E.: Optimal design of material properties and material distribution for multiple loading conditions. International Journal for Numerical Methods in Engineering **38**(7), 1149-1170 (1995)
20. Luo, Z., Yang, J., Chen, L.-P., Zhang, Y.-Q., Abdel-Malek, K.: A new hybrid fuzzy-goal programming scheme for multi-objective topological optimization of static and dynamic structures under multiple loading conditions. Structural and Multidisciplinary Optimization **31**(1), 26-39 (2006)
21. Sui, Y.K., Du, J.Z., Guo, Y.Q.: Topological optimization of frame structures under multiple loading cases. In: Computational Methods. pp. 1015-1022. Springer, (2006)
22. Balamurugan, R., Ramakrishnan, C.V., Swaminathan, N.: Integrated optimal design of structures under multiple loads for topology and shape using genetic algorithm. Engineering Computations **23**(1), 57-83 (2006)
23. Yulin, M., Xiaoming, W.: A level set method for structural topology optimization with multi-constraints and multi-materials. Acta Mechanica Sinica **20**(5), 507-518 (2004)
24. Wang, M.Y., Wang, X.: "Color" level sets: a multi-phase method for structural topology optimization with multiple materials. Computer Methods in Applied Mechanics and Engineering **193**(6-8), 469-496 (2004)
25. Allaire, G., Dapogny, C., Delgado, G., Michailidis, G.: Multi-phase structural optimization via a level set method. ESAIM: Control,Optimisation and Calculus of Variations **20**, 576-611 (2013)
26. Han, S.-Y., Lee, S.-K.: Development of a Material Mixing Method Based on Evolutionary Structural Optimization. JSME International Journal Series A **48**(3), 132-135 (2005)
27. Wang, M.Y., Zhou, S.: Synthesis of shape and topology of multi-material structures with a phase-field method. Journal of Computer-Aided Materials Design **11**(2-3), 117-138 (2005)
28. Ramani, A.: A pseudo-sensitivity based discrete-variable approach to structural topology optimization with multiple materials. Structural and Multidisciplinary Optimization **41**(6), 913-934 (2009)
29. Du, Z., Guo, X.: Variational principles and the related bounding theorems for bi-modulus materials. Journal of the Mechanics and Physics of Solids **73**, 183-211 (2014)
30. Achtziger, W.: Truss topology optimization including bar properties different for tension and compression. Structural Optimization **12**(1), 63-74 (1996)
31. Chang, C., Zheng, B., Gea, H.: Topology optimization for tension/compression only design. In: Proceedings of the 7th world congress on structural and multidisciplinary optimization 2007, pp. 2488-2495
32. Cai, K.: A simple approach to find optimal topology of a continuum with tension-only or compression-only material. Structural and Multidisciplinary Optimization **43**(6), 827-835 (2011)
33. Querin, O.M., Victoria, M., Martí, P.: Topology optimization of truss-like continua with different material properties in tension and compression. Structural and Multidisciplinary Optimization **42**(1), 25-32 (2010)
34. Cai, K., Gao, Z., Shi, J.: Topology optimization of continuum structures with bi-modulus materials. Engineering Optimization **46**(2), 244-260 (2013)
35. Qin, Q.H., Wang, H.: Matlab and C programming for Trefftz finite element methods. New York: CRC Press, (2008)
36. Martin, H.C., Carey, G.F.: Introduction to Finite Element Analysis: Theory and Applications. McGraw-Hill Book Company, New York (1973)

37. Qin, Q.H.: Hybrid-Trefftz finite element method for Reissner plates on an elastic foundation. Computer Methods in Applied Mechanics and Engineering **122**(3-4), 379-392 (1995)
38. Qin, Q.H.: Solving anti-plane problems of piezoelectric materials by the Trefftz finite element approach. Computational Mechanics **31**(6), 461-468 (2003)
39. Qin, Q.H.: The Trefftz finite and boundary element method. WIT Press, Southampton (2000)
40. Qin, Q.H.: Trefftz finite element method and its applications. Applied Mechanics Reviews **58**(5), 316-337 (2005)
41. Svanberg, K.: The method of moving asymptotes—a new method for structural optimization. International journal for numerical methods in engineering **24**(2), 359-373 (1987)
42. Ansys: ANSYS. (2012).
43. Cai, K., Qin, Q.H., Luo, Z., Zhang, A.J.: Robust topology optimisation of bi-modulus structures. Computer-Aided Design **45**(10), 1159-1169 (2013)